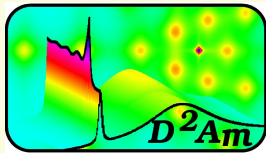


# XPAD : an hybrid pixel detector for material sciences studies using X-ray synchrotron radiation.

J.-F. Bérar, S. Arnaud, S. Basolo, N. Boudet, P. Breugnon, B. Caillot, J.-C. Clemens, P. Delpierre, B. Dinkespiler, S. Hustache, I. Koudobine, M. Menouni, P. Pangaud, R. Potheau, E. Vigeolas



D2AM/CRG-ESRF  
Grenoble



LdC-CNRS



SOLEIL  
St Aubin



CPPM-IN2P3-CNRS  
Marseille

Feb. 17th, 2006



Campinas sincrotron

# Summary.

- Detectors & material sciences scattering 3
- XPAD project and prototypes 6
- Resolution, dynamical range, . . . 10
- XPAD2 calibration and dispersion 13
- SAXS application 16
- Powder diffraction application 18
- Kinetics potentiality 21
- Multilayer studies 23
- from XPAD2 to XPAD3 25

# Detectors & material sciences scattering

**Imaging** : → X-ray microscopy, X-ray topography, X-ray radiography

**Spectroscopy** : chemical composition (XAS), short order range (EXAFS)

**Scattering** by beam →  $I(Q) \propto F^2(\rho)_e$

## Intensity range in scattering experiments

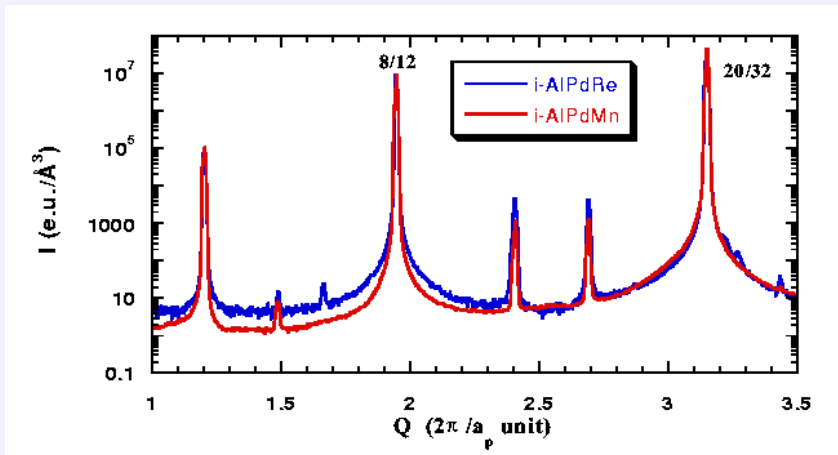
$1 \rightarrow 10^4$	13b	mean structure	chemistry (biocrystallography)
$1 \rightarrow 10^6$	20b	ordering	correlation, incommensurate
$1 \rightarrow 10^9$	30b	SAXS	$\mu m$ objects interaction, polymers

- Synchrotron → current flux on sample :  $10^{11} - 10^{14} \nu/s$
- Spot size at sample or detector position :  $1 \times 5 \rightarrow 0.05 \times 0.10 mm^2$
- Counting rate :  $10^9 \nu/s$  within  $10^{-2} mm^2$
- Resolution : angular  $10^{-3}^\circ \rightarrow 100 \mu m$  at  $0.5 m \approx 0.01^\circ$

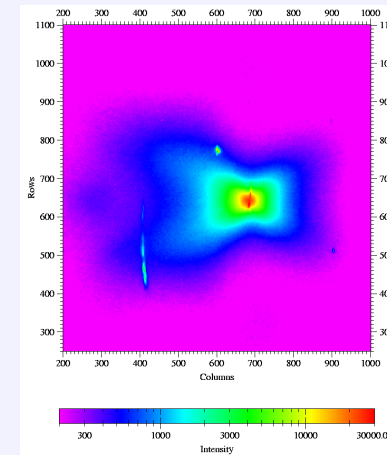
# On D2AM-CRG/ESRF beamline (BM2).

Very demanding experiments use slits and photomultipliers to reach the required quality.

In structural works, CCD cameras with indirect photon detection are commonly used.



Diffuse scattering in icosahedral quasi-crystals : 7 orders of magnitude are necessary to measure this signal. Dynamic extended by **attenuators**, time consuming mapping



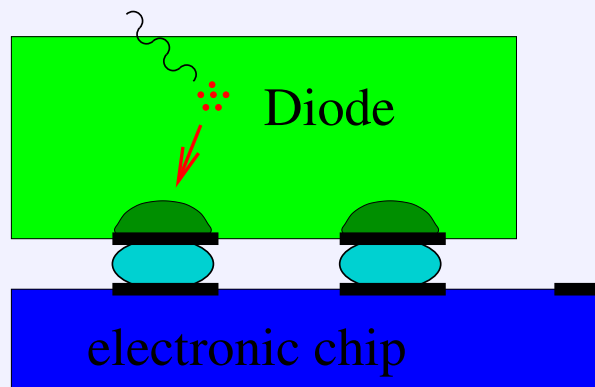
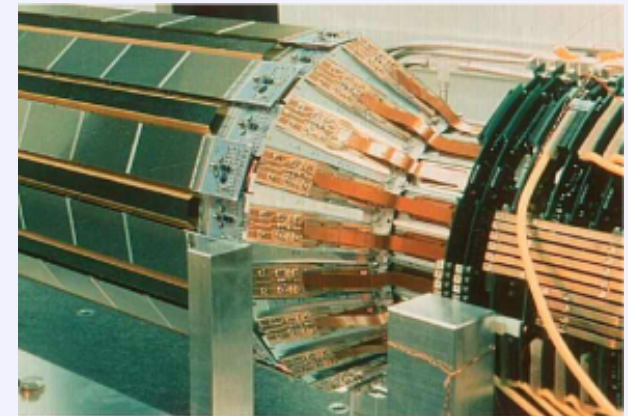
Complex shape of the diffusion around Bragg peak obtained by adding 10 (1000) frames. Out of peak to avoid blooming effects

Data from M. de Boissieu, see Phil. Mag. Let. (2001) 81, 273-283 and (2003) 83, 1-29

# D2AM-CRG/ESRF detector requirement

dynamic range	$> 10^9 \text{ count/pixel}$	$\Rightarrow 32 \text{ bits architecture}$
saturation rate	$> 10^7 \nu/s/pixel$	$\Rightarrow \text{noise} < 0.1 \nu/s/pixel$
energy range	$5 \rightarrow 25 \text{ keV}$	from beamline
pixel size	$250 \times 400 \mu\text{m}^2$	mean spot size in 1995
exposure time	$1 \text{ ms} \rightarrow 1000 \text{ s}$	kinetics potentiality

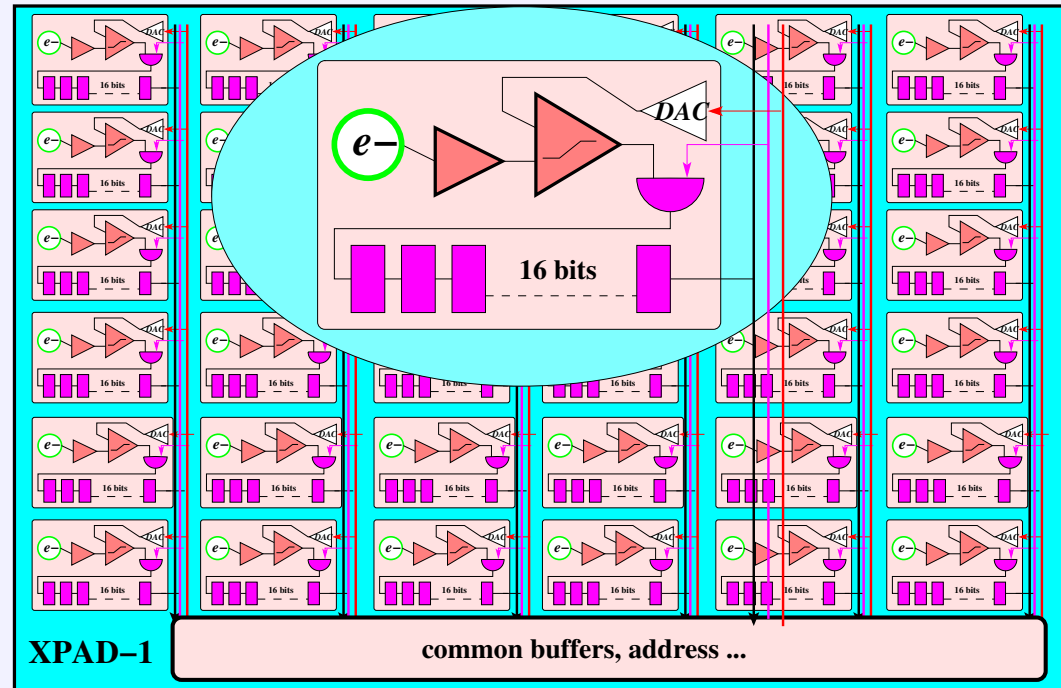
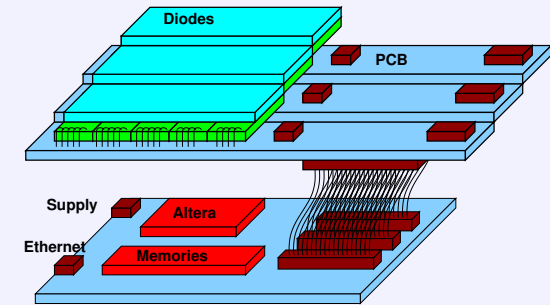
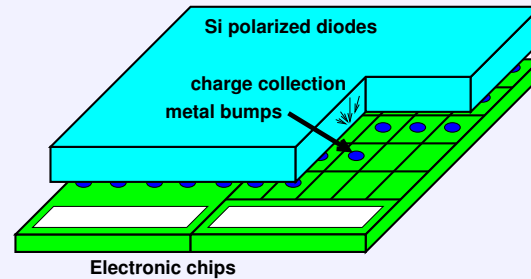
High energy physics experiments lead to built detector like Delphi at CERN which uses the potentiabilities offered by microelectronics and direct photon conversion in silicon.



The silicium thickness  $300 \mu\text{m}$  and the pixel sizes  $330 \times 330 \mu\text{m}^2$  were convenient to our beamline requirements leading to the project of building a new X-ray detector taking benefit of the Delphi detector peoples knowledge.

# The XPAD project (XPAD1).

- Absorbed photons
- electron clouds
- charge migration
- electron bunches
- pixel threshold
- pixel counters
- on-board memories
- ethernet data



Diodes :

- high resistivity Si

Chips :

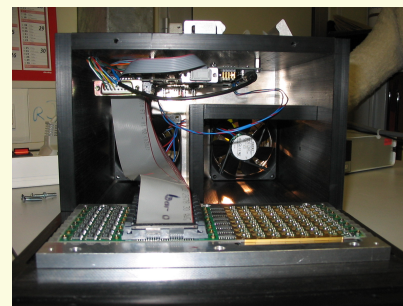
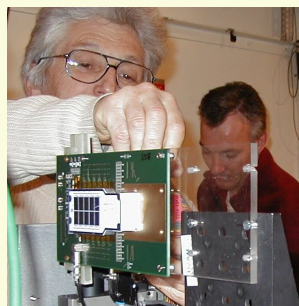
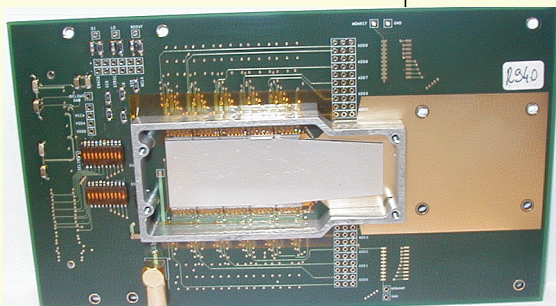
- AMS CMOS  $0.8 \mu m$
- $24 \times 25$  pixel/chip

Boudet *et al.*, NIM A510 (2003) 41-44,

Berar *et al.*, J. Appl. Cryst. 35 (2002) 471-476

# XPAD detectors.

	<b>XPAD1</b> 2001	<b>XPAD2</b> 2003	<b>XPAD3</b> 2006
pixel size	330 x 330 $\mu m$		130 x 130 $\mu m$
foundry	AMS 0.8 $\mu m$ CMOS		IBM 0.25 $\mu m$
pixel / chips	24 x 25 pixels		80 x 120 pixels
internal counters	16 bits		14 bits
overflow counters	16 bits		16 bits
energy range	15 to 25 keV		7 to 25 keV
sensor	Si 300 $\mu m$ (Delphi)	Si 500 $\mu m$	
counting rate	$1.10^6 ph/s$	$2.10^6 ph/s$	$2.10^5 ph/s$
time constant	500 ns with detector	208 ns with detector	<i>to be measured</i>
modules	5 x 2 chips	8 x 1 or 8 x 8 chips	8 x 7 chips
detector	1 module	up to 8 modules	
electronic connection	reduced parallel wires	back plugged ethernet 100MB	

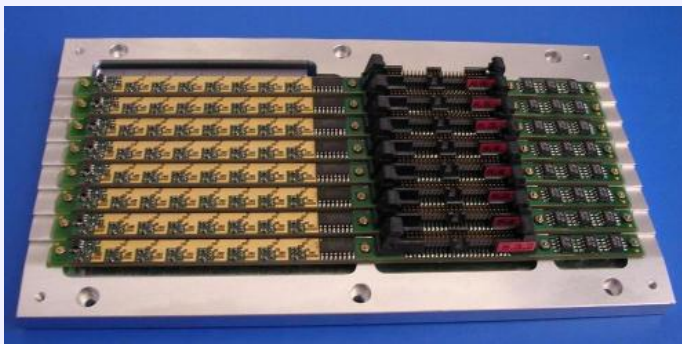
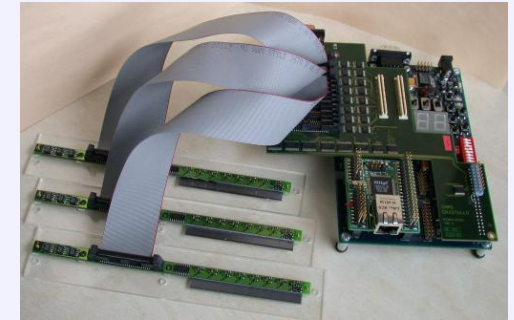


# XPAD2 detector : 8 modules $\times$ 8chips

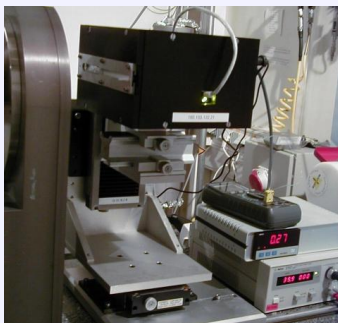
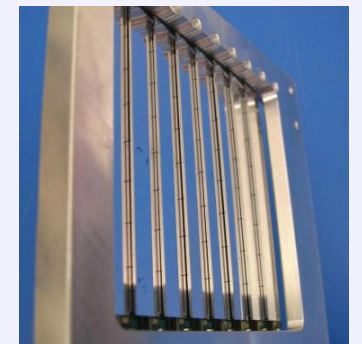
New diodes of  $500\mu\text{m}$  Si thick  $\rightarrow$  efficiency 78 % @15keV, 21% @25keV



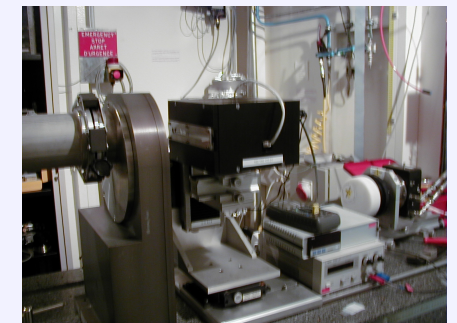
Diode  $\Rightarrow$  8 chips of  $24 \times 25$  pixels  
PCB card : drivers and regulators.  
Modules  $\Rightarrow$  acquisition card  
Altera Nios kit + ethernet



Tiled as close as possible  
 $\rightarrow$  reduce shading, dead zones.  
Metallic holder  $\rightarrow$  few  $\mu\text{m}$ .  
Size :  $200 \times 192$  pixels  
Surface  $\approx 68 \times 68\text{mm}^2$ .



Interface software  
developed using LabWindows/CVI  
application software moves to Linux.  
XPAD prototype at SAXS station.



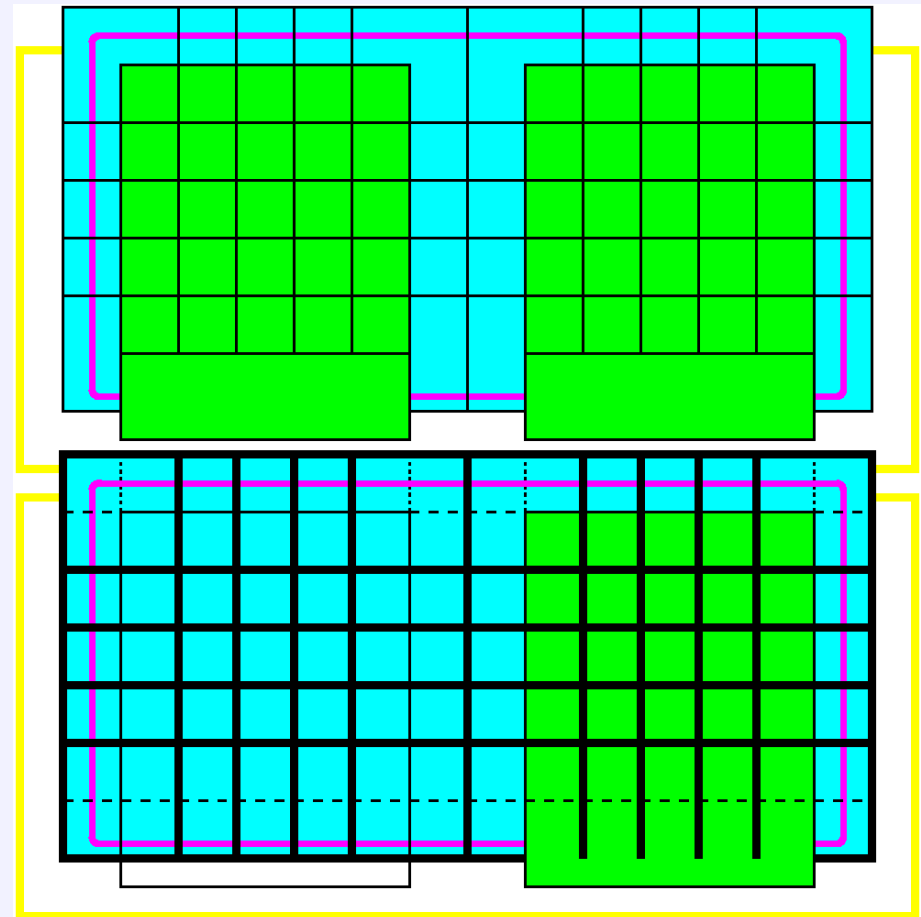


# Dead area in pixel detectors

The mechanical structure of such detector induces some dead area, it seems necessary to minimize it or at least to know it.

**Within modules** : No dead area  
Pixels at the border of the chip are connected to pixel diode with an increased surface to avoid dead area associated with the packing of chips on the detector : mechanical border, guards ring...

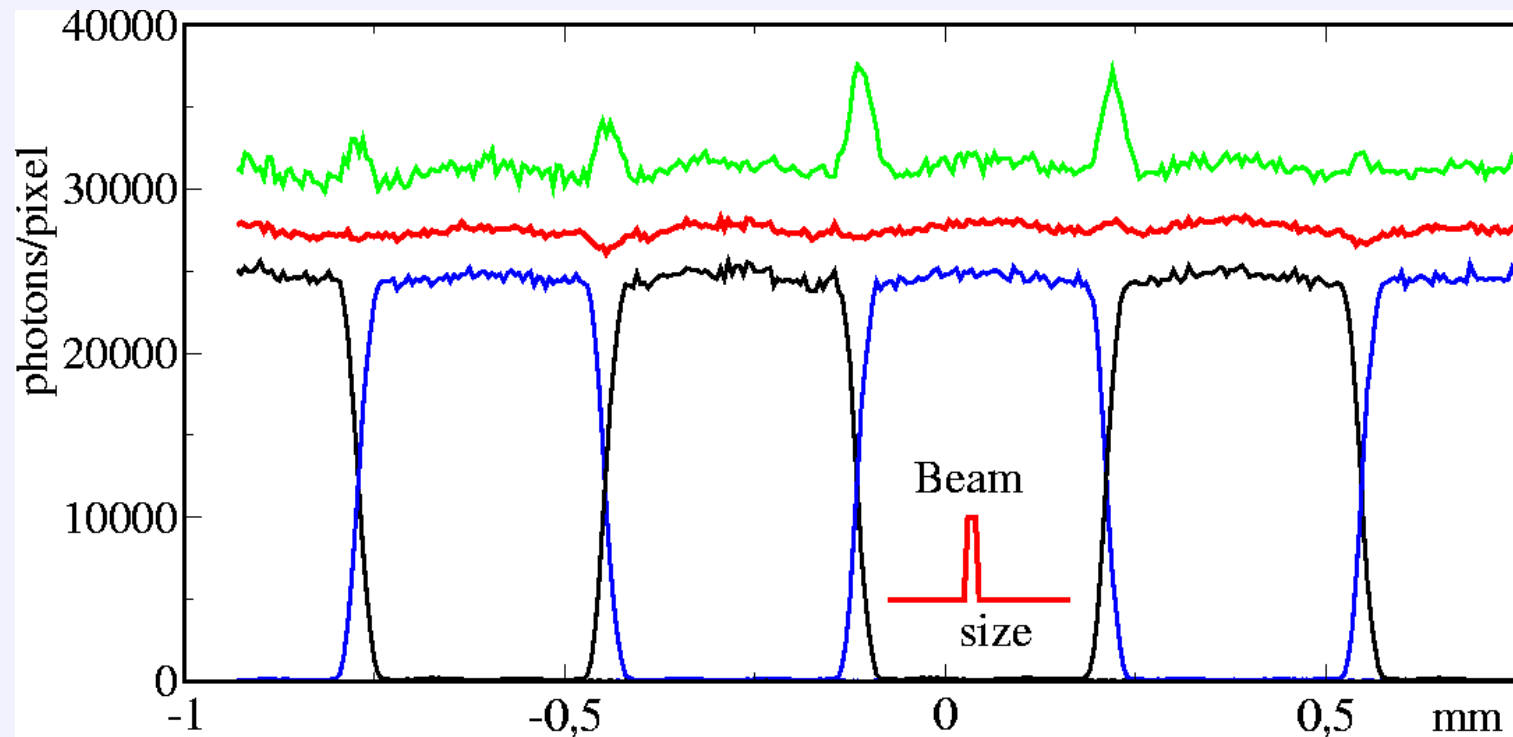
**Between modules** :  $\approx 1$   
pixel/column  $\Rightarrow 4\%$  XPAD2  
 $\rightarrow 1\%$  XPAD3



# Spatial resolution

As the diode is common to pixels belonging to the same chip, some charge sharing may occur between adjacent pixels.

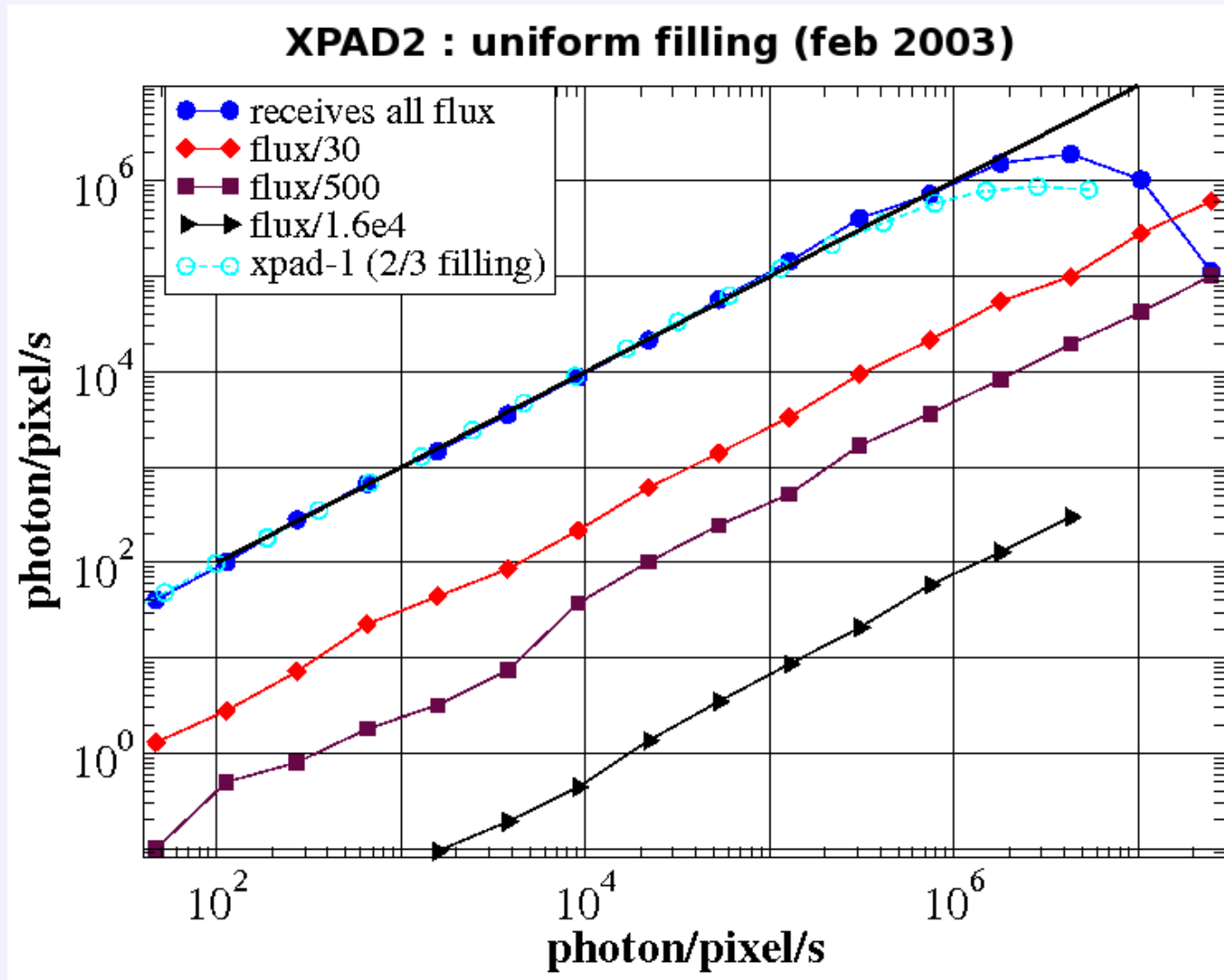
Measurements show that the charge sharing occurs on  $\approx 60 \mu m$ .



A flat field can be obtained when energies edge is perfectly adjusted in each pixel (red). In case of too low edges, this share sharing create some over-counting at pixel borders (green).

# Dynamical range

Counts in adjacent pixels as a function of the incoming flux.

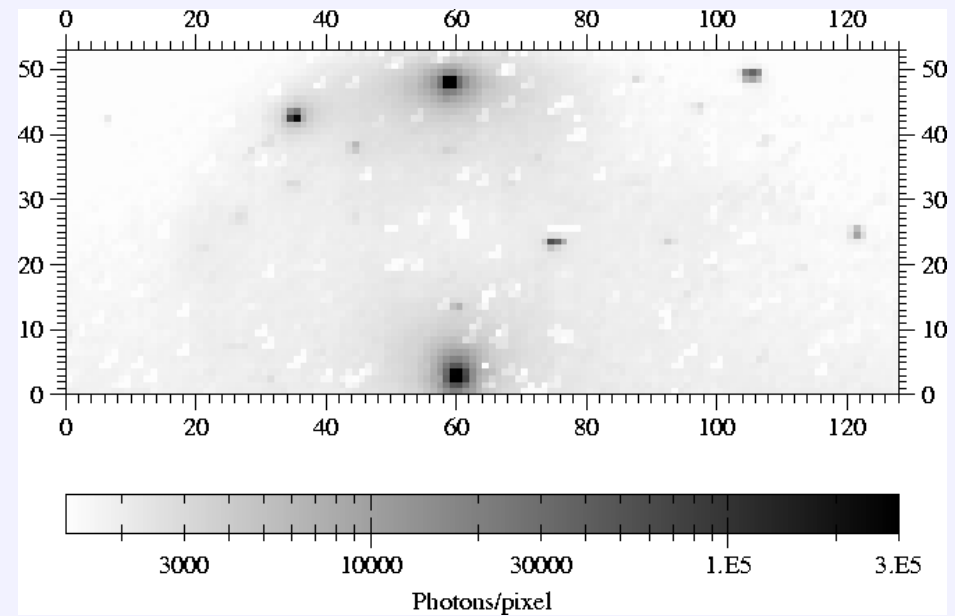
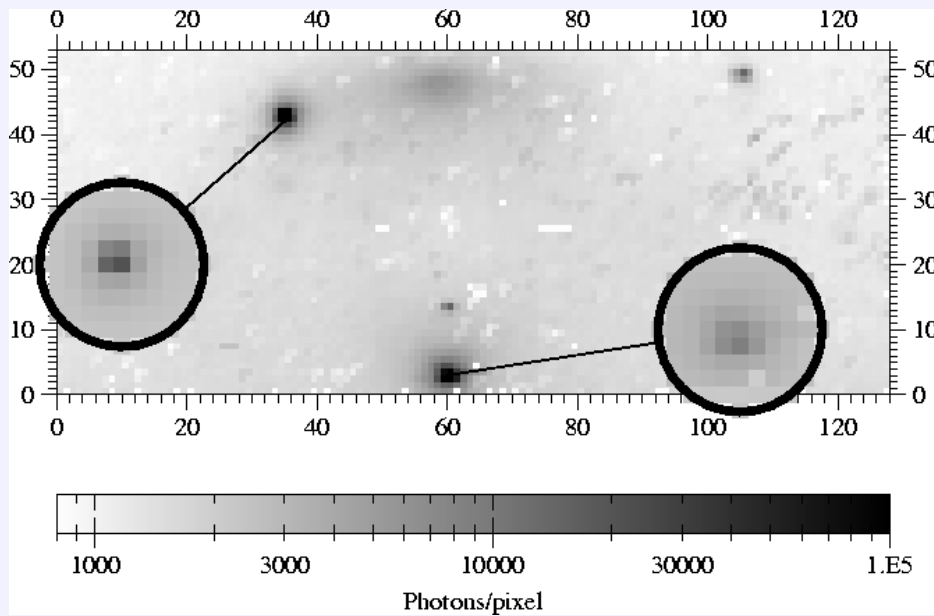


No blooming effect

- Overall dead time  $\approx 0.21\mu s$
- Xpad chip dead time  $< 0.10\mu s$

# Dynamical range (XPAD1 application)

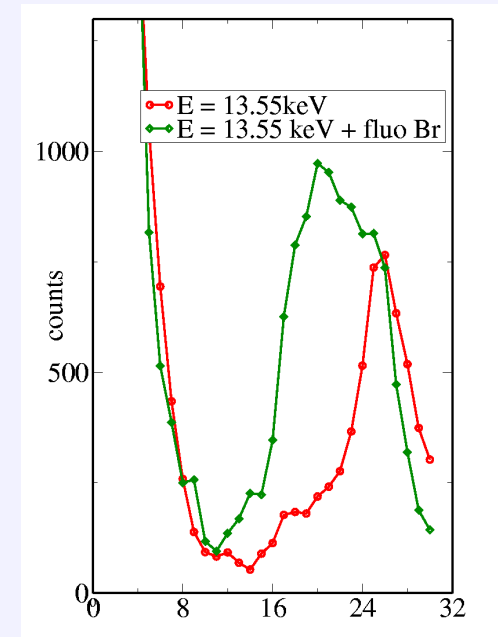
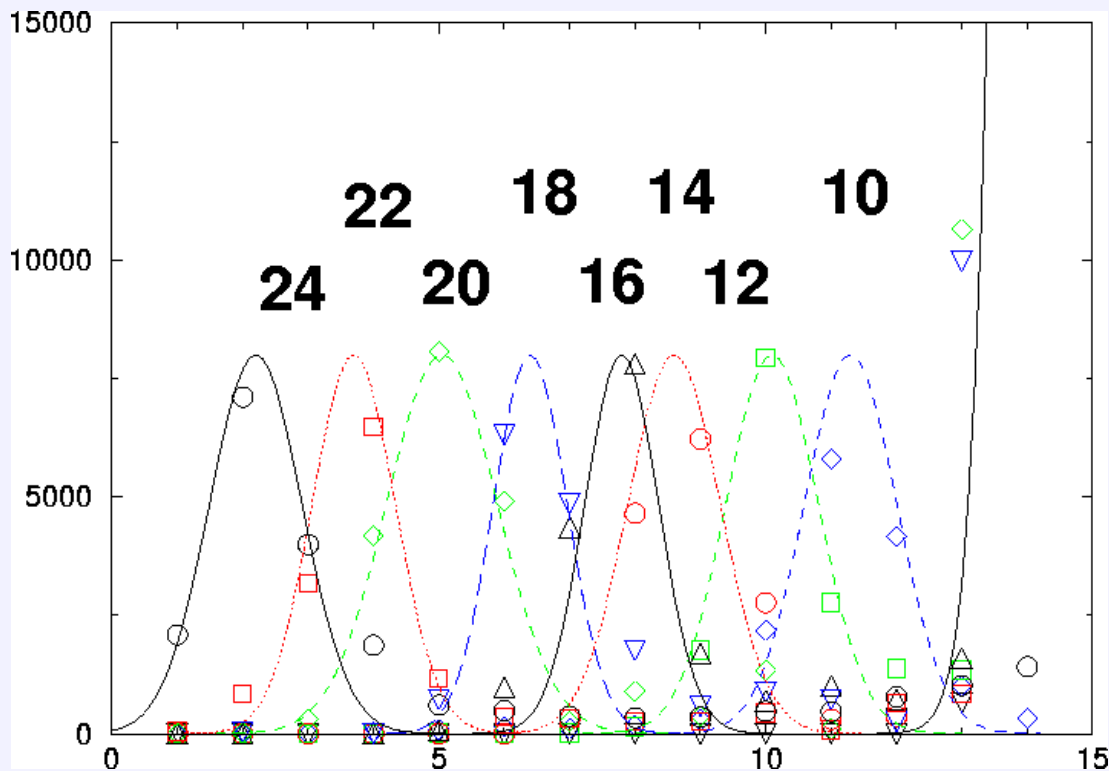
Diffusion (left) of a CdYb icosahedral quasicrystal and associated rotation image (right) on which the highest peak is near counter saturation rate, it cross the Ewald sphere within a few part of the exposure!



*To obtain similar images with CCD cameras : attenuator are required and a few hundred images have to be summed.*

# Energy resolution

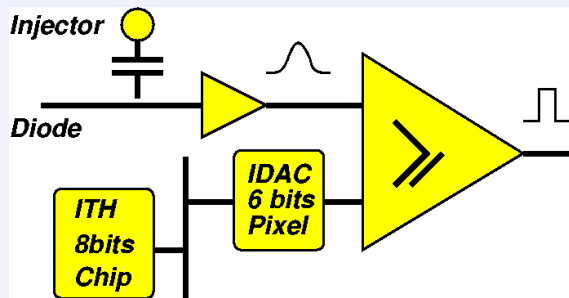
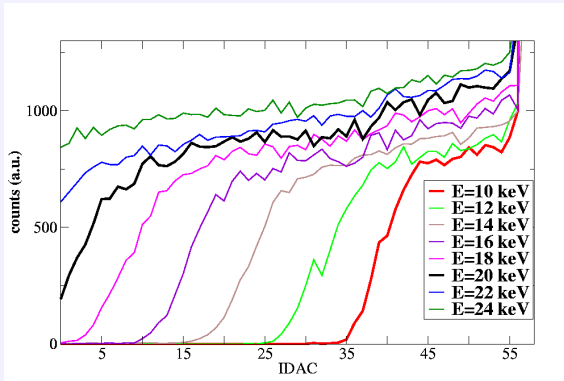
The conversion of incoming photons in silicon leads to a charge proportional to the incoming energy. The XPAD chip energy resolution is near  $1\text{ keV}$ .



Measured counts as a function of the threshold for the diffusion of a Br solution on both sides of Br absorption edge.

Pixel threshold register : 4 bits (XPAD1)  $\rightarrow$  6 bits (XPAD2)

# XPAD2 calibration and dispersion (1)



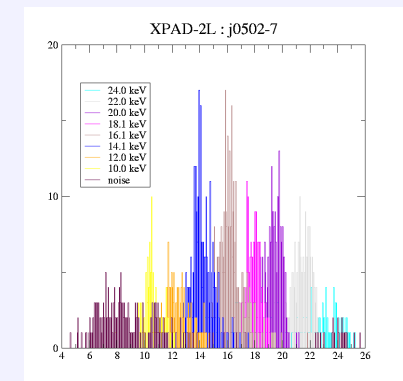
- *beam*  $E_x$  : monochromatic flat scattering (amorphous), noisy, time expensive
- *injection*  $E_{inj}$  : simulate the beam, quick and easy but need calibration
- Each pixel is described by :  $C, \alpha, \beta, E_{inj}(noise)$   

$$E_x = C E_{inj} = \alpha(I_{th}) + \beta(I_{dac})$$

$$E_x(noise) = C E_{inj}(noise)$$
- $\approx 4 \cdot 10^4$  pixels  $\Rightarrow$  automatic configuration/calibration procedure.

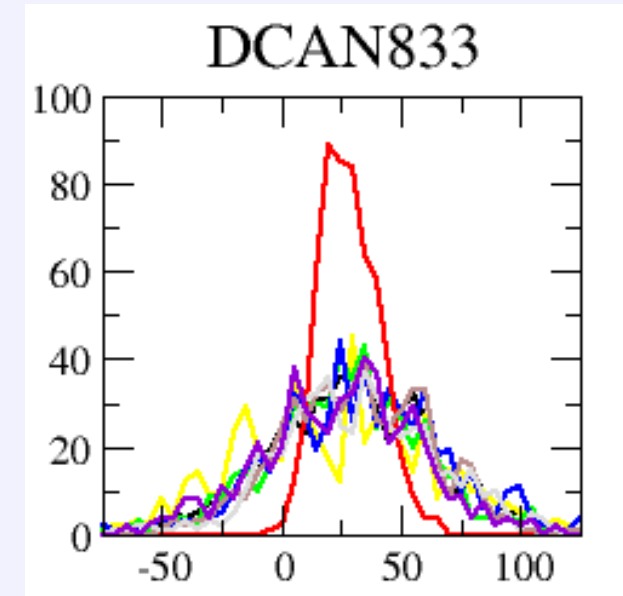
Knowing then these characteristics :

the setup of each chip at a given energy  $E$  can be defined as the value of the chip common threshold level  $I_{th}$  for which most of the pixels can be fine tune,  $I_{dac} \in [0, 63]$ .



# XPAD2 calibration and dispersion (2)

- XPAD2 initial threshold dispersion  $60 e^-$   
⇒ pixels not tuned  $< 3\%$
- manufacturing problems :  
leakage in bumping process  
⇒ new foundry using the same masks
- threshold dispersion increase strongly  
 $\approx 120 e^-$  on most chips  
⇒ pixels not tuned  $< 15\%$

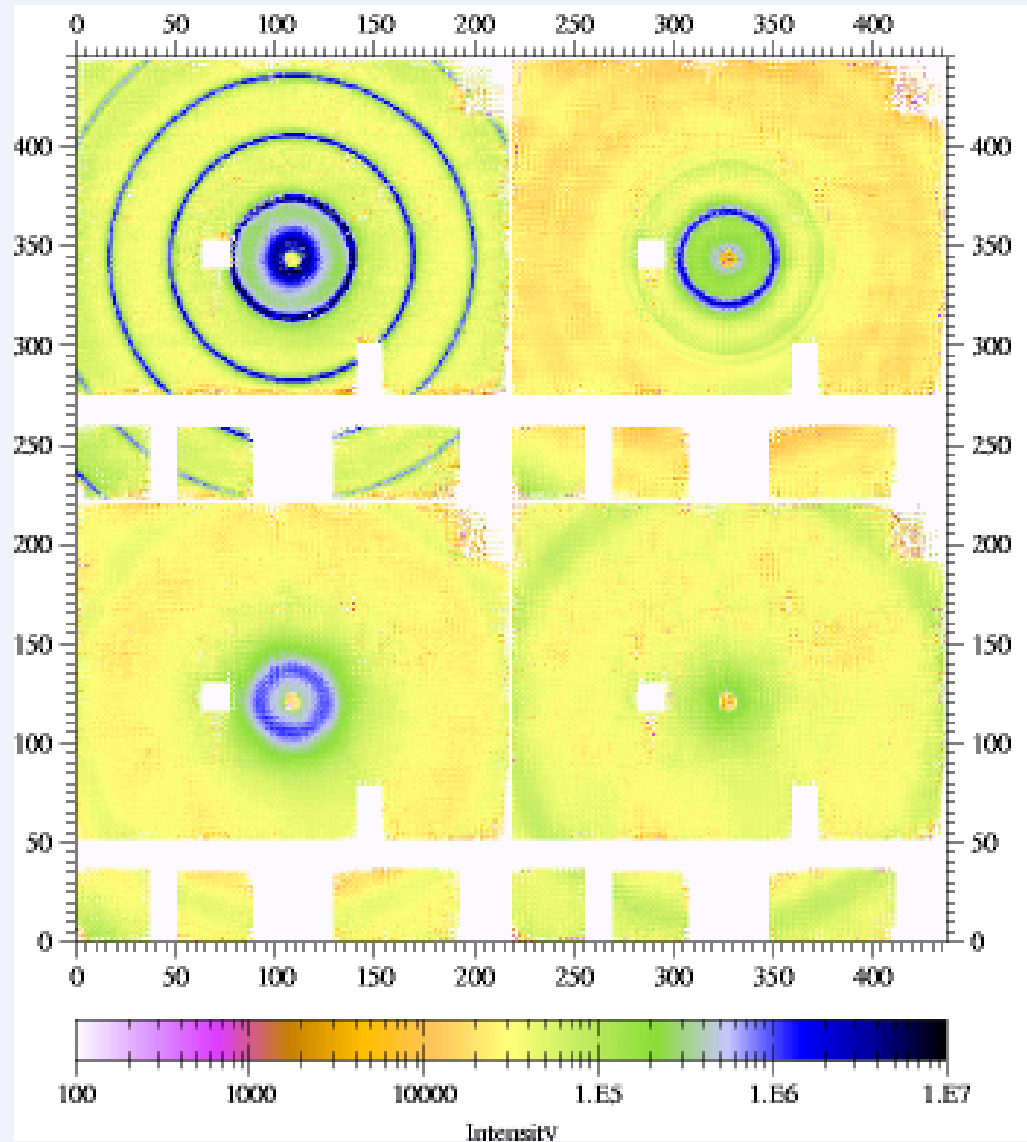


However, even if all the pixels are not perfectly set, the XPAD2 detector appears as a usefull tool for recording new data in SAXS and diffraction on a synchrotron beamline in the range 15 - 25 keV.

# SAXS application (1)

Scattering of some samples recorded at BM2-SAXS camera using XPAD detector at 20 *keV*.

- Ag Behenate
- Bee waxes
- Polyurethan
- Empty cell
- Teflon
- Water (5mm)

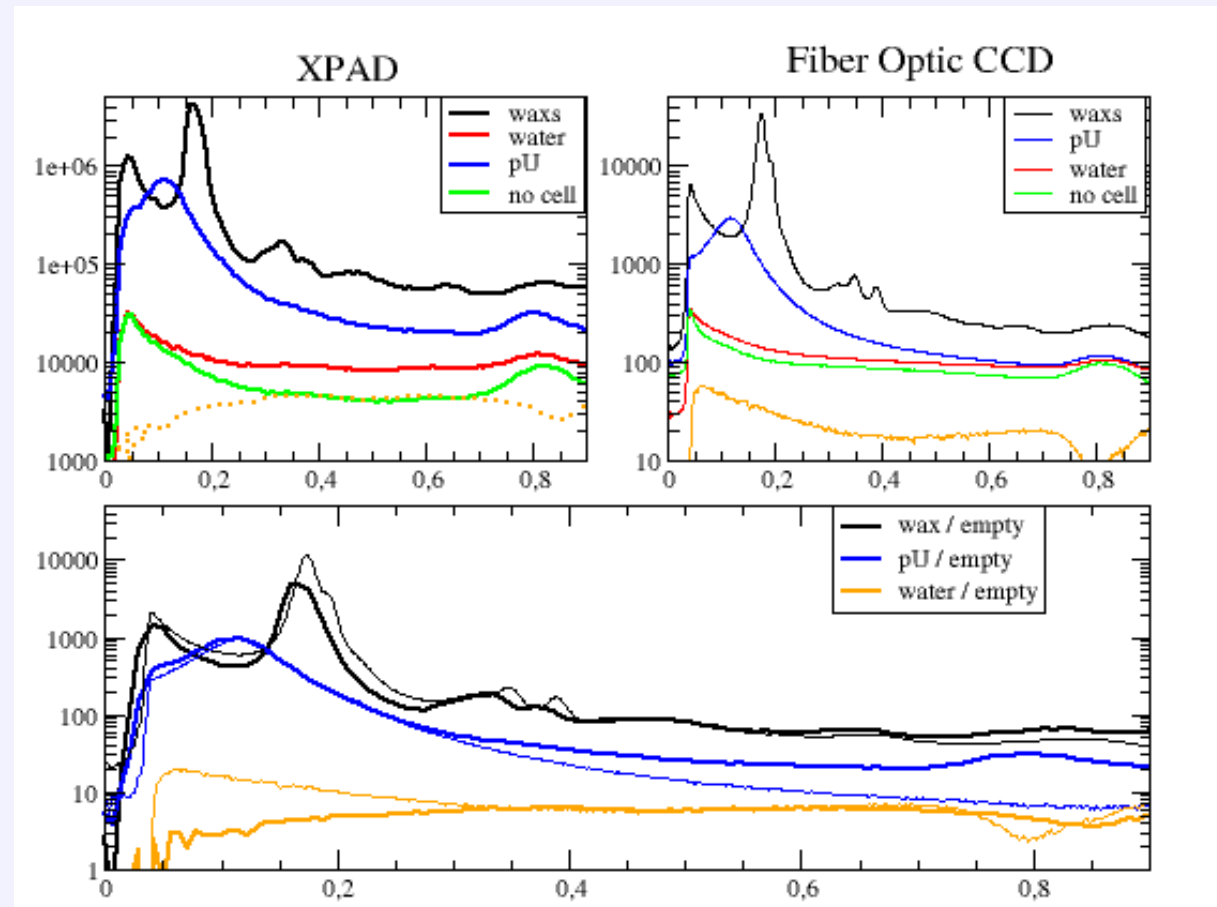




# SAXS application (2)

Data have been compared with FOB CCD\* ones using the same setting.

The low noise achieved with the XPAD detector allows to improve the measurement of weak scatterer like water : the signal observed without sample is really lower with XPAD than with the CCD (fluorescence, PSF tails ...)

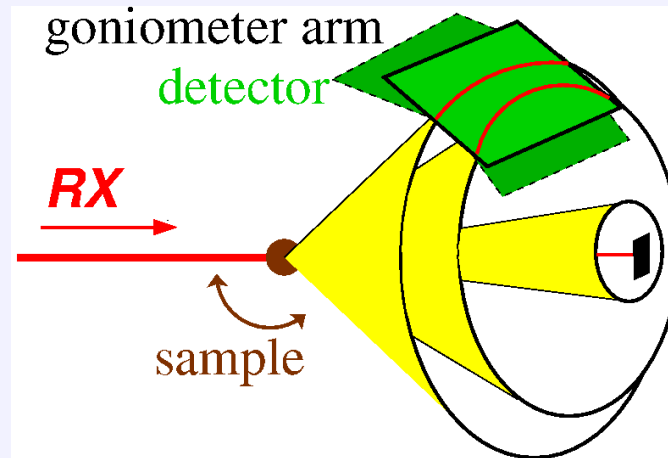
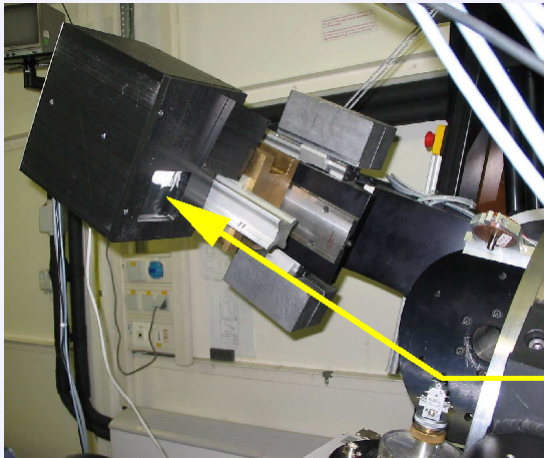


\* PI-SCX-1300, Roper Scientific (EEG 1340x1300, 50 $\mu$ m pixel size, dark corrected)

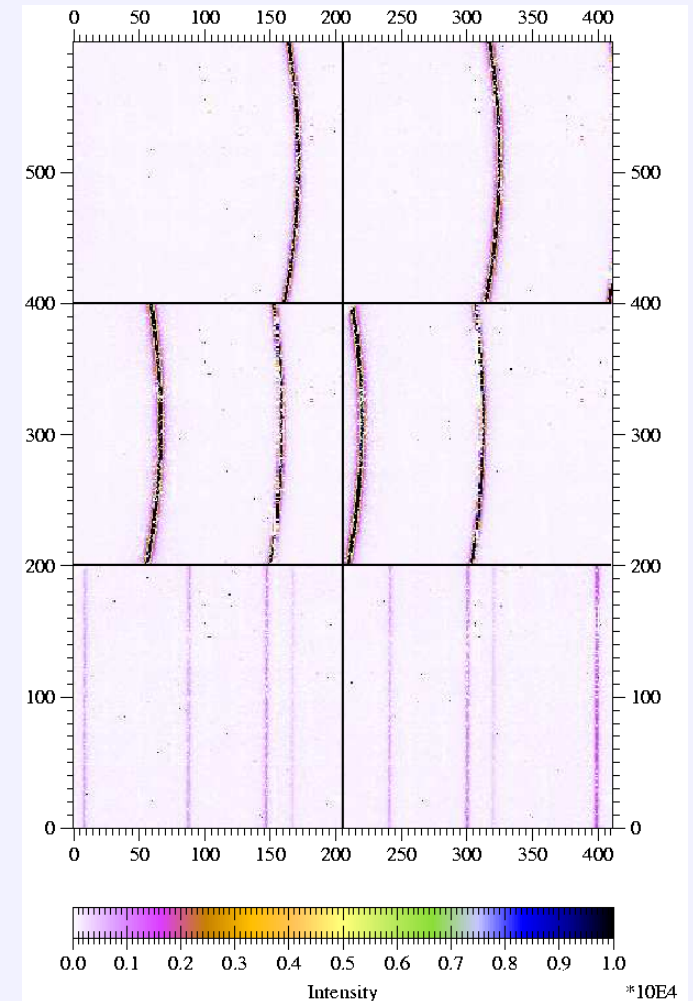
# Powder diffraction application (1)

Scintillator and slits → 2d-detector.

- Diffraction along cones
- Data redundancy with 2D detector
- $60^\circ$  collected at high resolution
- angular aperture  $4^\circ$  at  $1m$



With 0-D detector pipes and slits remove diffuse scattering, background level partly removed with conic pipes on 2d-detector.



Raw images with Bragg lines, low and high angles.

# Powder diffraction application (2)

Reconstructed Debye-Scherrer film  
or powder pattern

Resulting counts  $Y$  on pixel  $p$  :

$$Y_p = N_p^{-1} \sum f_q y_{q,i}$$

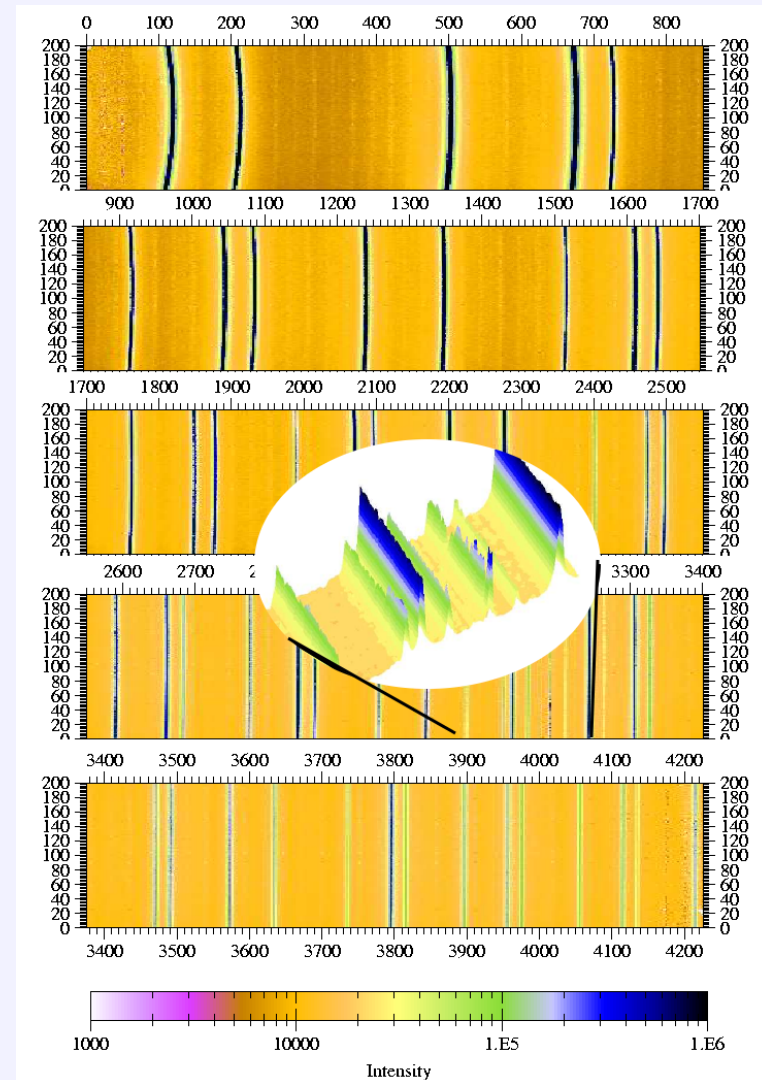
$y_{q,i}$  counts on image  $i$  of pixel  $q$ ,  
 $f_q$  flatfield of pixel  $q$  :

Film :  $q \in Image_i \rightarrow p \in Image_{merged} : q = q(p, i)$

Minimisation:  $\sum_p (Y_p - N_p^{-1} \sum_i f_q y_{q,i})^2$

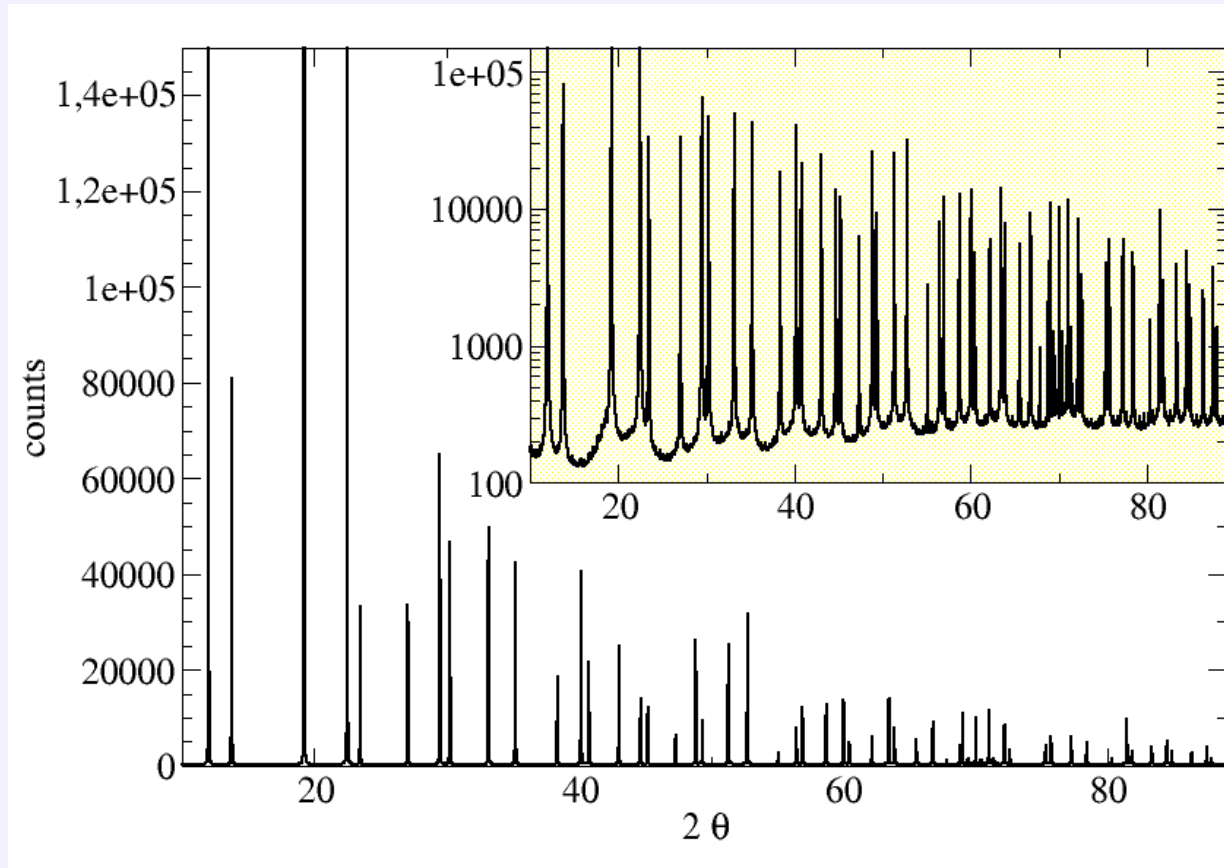
Powder lines :  $Y_{p \in Ring} \rightarrow Y_{Ring}$

$$\sum_{Ring} (Y_{Ring} - N_{Ring}^{-1} \sum_{p \in Ring} \sum_i f_q y_{q,i})^2$$

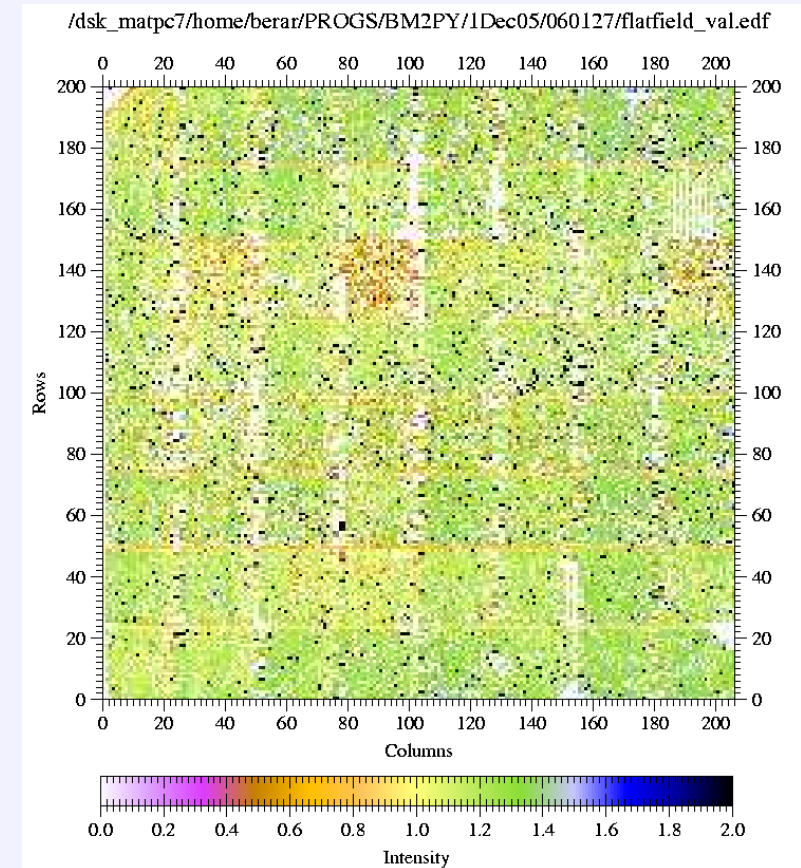


# Powder diffraction application (3)

Reconstructed powder pattern



flatfield extraction

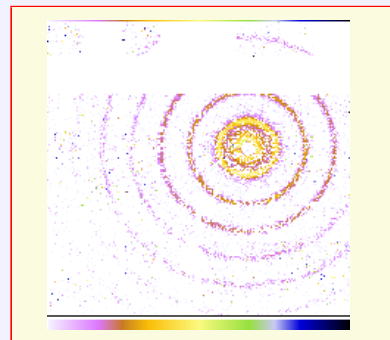
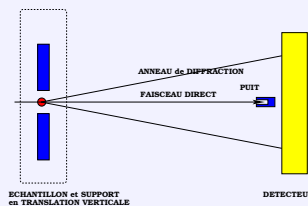
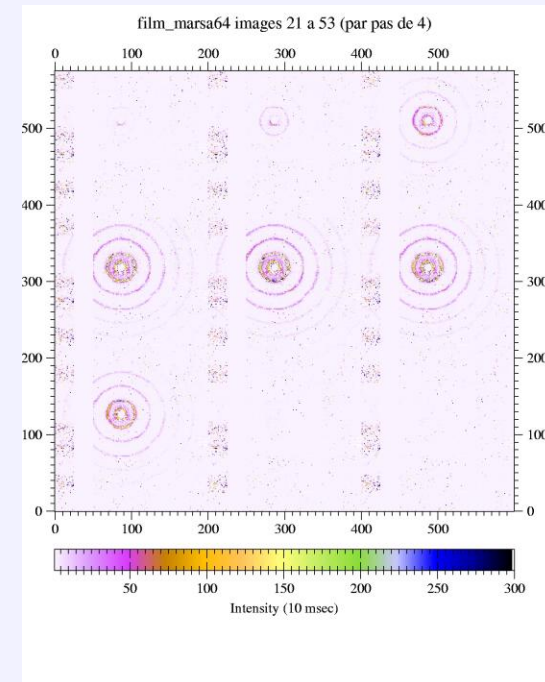


As shown with log scale, high quality data are obtained at high angles. Last detector assembly exhibit a quite uniform flatfield at 20 keV, even if pixels have not be very accutely tuned.

# Kinetics potentiality of XPAD2

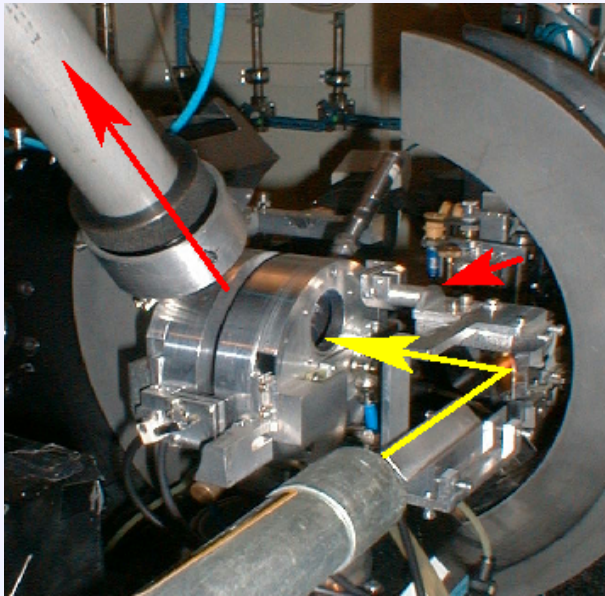
Whole electronic designed to allow kinetics studies (ms range)

- chips register 16bits + overflow
- on-board memories 32 bits
- exposure time :  $1ms \rightarrow 8300s$
- dead time for reading :
  - whole image  $2ms$
  - overflow  $16\mu s$  each  $10ms$
- on-board storage :
  - 423 images  $< 10ms$
  - 233 images  $\geq 10ms$

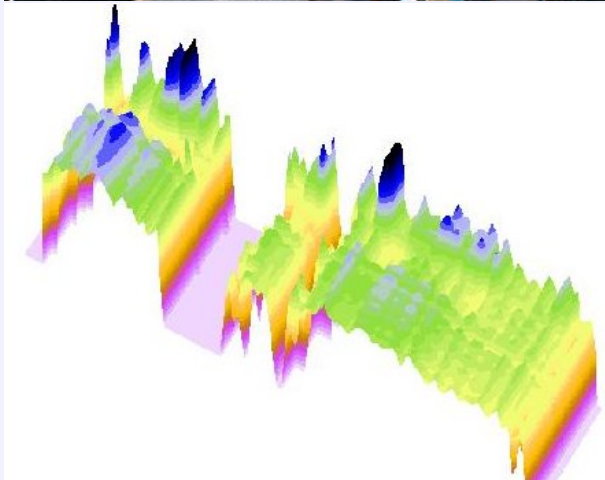
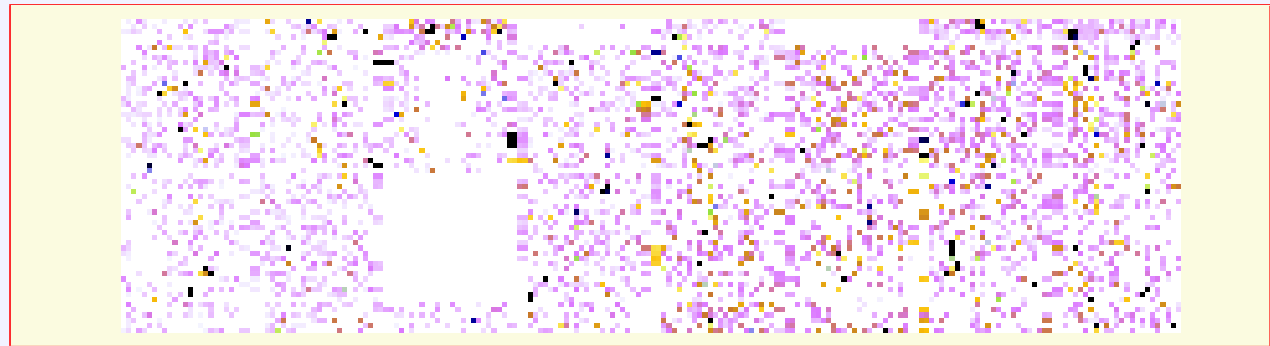


Images of 10 ms each taken of a 2s movies showing diffraction while the sample crosses the beam at D2AM SAXS camera.

# Kinetics of quench studied by diffraction



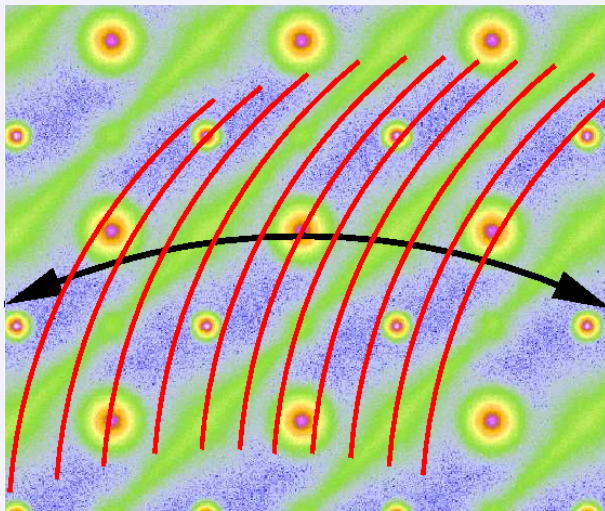
Data collection is limited by the cell aperture, which has been designed for linear detector, a few frames of 20ms around crystallisation shown at 10 frames/s.



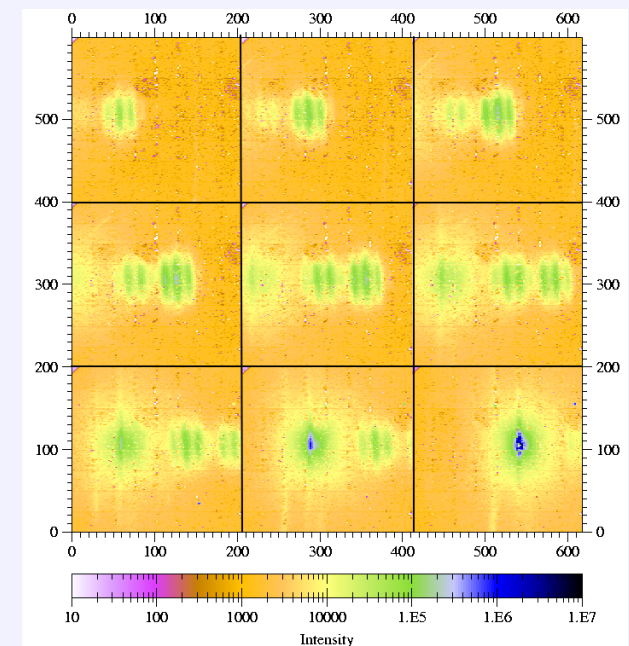
The quench of  $Al_{2x}Ca_yO_{3x+y}$  ceramics can lead to vitreous or crystalline oxides. The transition between the liquid state and the crystalline one occurs in less than 20ms and may exhibit some transient phases.

# Multilayers

Epitaxially grown multilayer are now common samples to characterize : they need mapping of the reciprocal space which is time consuming. At the time such maps are recorded with slits and fixed  $(h, k, l)$  point of the reciprocal lattice, attenuators are often required near the substrate.



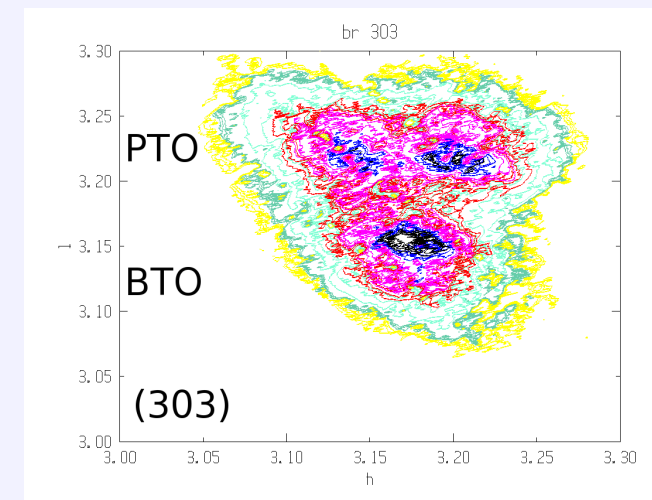
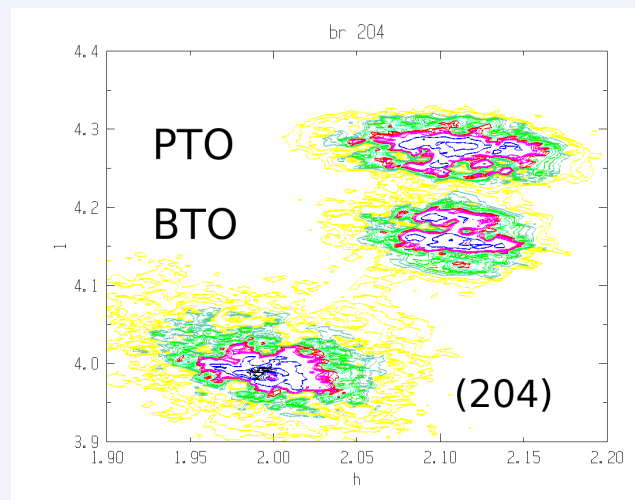
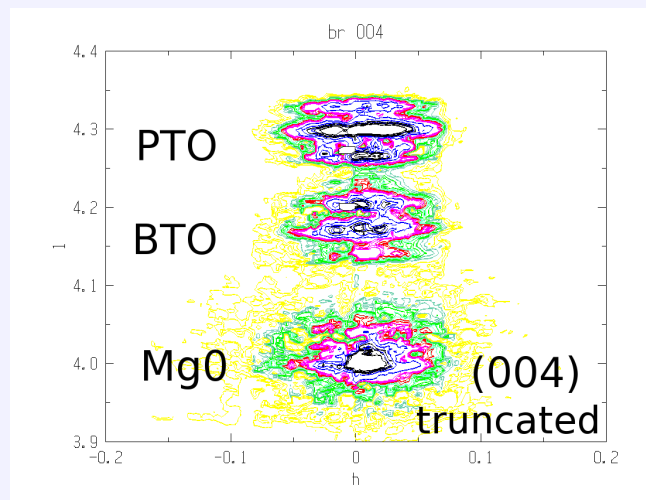
2-D detection allows an important improvement in these acquisitions but it needs to be able to manage high dynamics and to transform your reciprocal slices or volumes into reciprocal maps.



# Multilayers : Ferroelectric superlattice

27 (17 PbTiO<sub>3</sub>,17 BaTiO<sub>3</sub>) superlattice / MgO :  
large lattice mismatch → in-plane polarization → tetragonal distortion.

Physical behaviour of such compounds is primarily dependent on their epitaxial crystalline quality, their composition and their structural perfection.



Out of plane : strain / chemical

In plane : 2 PTO domains tetragonal distortion

The reciprocal maps are recorded scanning the XPAD detector and rebuilt from the collected reciprocal slices. Compared to standard data collection the time can be reduced by 100. Intensity on substrate peak can reach  $10^9 \nu/s$  !

F. Lemarrec, E. Dooryhee and coll., IUCr (2005) Florence, Italy



# from XPAD2 to XPAD3

- Obsolescence of the AMS-CMOS  $0.8\ \mu\text{m}$  technology used for XPAD2
- A new XPAD3 using  $0.25\ \mu\text{m}$  technology with  $25\ \mu\text{m}$  bumps

	XPAD2	XPAD3	comments
polarization	both	$e^+$	2 chips : Si, CdTe
pixel size	$330\ \mu\text{m}$	$130\ \mu\text{m}$	
chip size	$8 \times 10\ \text{mm}^2$	$10 \times 15\ \text{mm}^2$	→ reduce tiling
counting rate	$2 \cdot 10^6\ \text{ph/s}$	$2 \cdot 10^5\ \text{ph/s}$	≡ count/surface
energy range	(5) $15 \rightarrow 25\ \text{keV}$	$7 \rightarrow 25\ \text{keV}$	new analog chain
pixels/chip	$24 \times 25 = 600$	$80 \times 120 \approx 1 \cdot 10^4$	
pixels/module	$8 \times 600 \approx 5 \cdot 10^3$	$\approx 1 \cdot 10^5$	
pixels/detector	$\approx 4 \cdot 10^4$	$\approx 5 \cdot 10^5$	
geometries	$8 \times 8$ or $2 \times 5$	$7 \times 8$ and ?	

- Chip design has been carried out
- Prototype is expected for mid 2006.